APPLIED GEOPHYSICS, Vol.12, No.1 (March 2015), P. 47-54, 11 Figures.
DOI: 10.1007/s11770-015-0467-3

Random noise attenuation by *f–x* spatial projection-based complex empirical mode decomposition predictive filtering*

Ma Yan-Yan[1,2], Li Guo-Fa[1,2], Wang Yao-Jun[1,2], Zhou Hui[1,2], and Zhang Bao-Jiang[3]

Abstract: The frequency–space (*f–x*) empirical mode decomposition (EMD) denoising method has two limitations when applied to nonstationary seismic data. First, subtracting the first intrinsic mode function (IMF) results in signal damage and limited denoising. Second, decomposing the real and imaginary parts of complex data may lead to inconsistent decomposition numbers. Thus, we propose a new method named *f–x* spatial projection-based complex empirical mode decomposition (CEMD) prediction filtering. The proposed approach directly decomposes complex seismic data into a series of complex IMFs (CIMFs) using the spatial projection-based CEMD algorithm and then applies *f–x* predictive filtering to the stationary CIMFs to improve the signal-to-noise ratio. Synthetic and real data examples were used to demonstrate the performance of the new method in random noise attenuation and seismic signal preservation.
Keywords: Complex empirical mode decomposition, complex intrinsic mode functions, *f–x* predictive filtering, random noise attenuation

Introduction

Predictive filtering in the frequency–space (*f–x*) domain (Canales, 1984; Gulunay, 1986; Abma and Claerbout, 1995), herein referred to as the FXdecon method, is a popular random noise attenuation method in real seismic data processing. This method assumes that signals are predictable in the *f–x* domain, whereas random noise is not. Random noise can be attenuated by combining the prediction filter operator with original seismic data in the *f–x* domain. There are two limitations in the FXdecon method. First, FXdecon predicts noise as source noise rather than additive noise. Soubaras (1994) used *f–x* projection filtering to remedy the inconsistency between source noise and additive noise. Sacchi and Kuehl (2001) used the autoregressive moving average model in place of the autoregressive model as the prediction filter to avoid this inconsistency. Trickett (2003) used the Cadzow filter to realize a filtering algorithm that can adapt to sloping and conflicting events (Yuan and Wang, 2011). Second, FXdecon

Manuscript received by the Editor February 24, 2014; revised manuscript received February 13, 2015.
*This work is supported financially by the National Natural Science Foundation (No. 41174117) and the Major National Science and Technology Projects (No. 2011ZX05031–001).
1. State Key Laboratory of Petroleum Resources and Prospecting, China University of Petroleum, Beijing 102249, China.
2. CNPC Key Laboratory of Geophysical Prospecting, China University of Petroleum, Beijing 102249, China.
3. Petroleum Exploration and Production Research Institute, SINOPEC, Beijing 100083, China.

cannot deal with nonstationary seismic data. Time–frequency analysis tools such as the wavelet transform (Ioup and Ioup, 1998) and curvelet transform (Wang et al., 2010) are used to solve the nonstationary problem in seismic data. However, these transforms need preset basic functions that lack clear physical significance and may lead to poor performance in practical applications. Battista et al. (2007) introduced the Hilbert–Huang transform (HHT) to seismic data processing. HHT uses the empirical mode decomposition (EMD) to decompose a nonstationary signal into a series of intrinsic mode functions (IMFs) without presetting any basic functions. Bekara and van der Baan (2009) used EMD instead of the prediction filter operator in the *f–x* domain to attenuate noise and proposed the FXEMD denoising method. This scheme decomposes the real and imaginary parts of the frequency slice using the EMD algorithm, subtracts the first IMF, and then stacks the residual parts to obtain the final denoised slice. However, there are two limitations in the FXEMD method. First, signals and noise coexist on all IMFs; thus, simply subtracting the first IMF will result in signal damage and limited denoising ability. Second, the respective decomposition of real and imaginary parts may destroy the unity structure of the complex signal and even lead to inconsistent decomposition numbers between real and imaginary parts.

We propose a novel method named *f–x* spatial projection-based complex empirical mode decomposition (CEMD) prediction filtering or FXCEMDdecon. First, we directly decompose nonstationary complex seismic data in the *f–x* domain into complex intrinsic mode functions (CIMFs) using the spatial projection-based CEMD algorithm, and then apply the FXdecon filter to the stationary CIMFs to attenuate noise. Synthetic and real seismic data are used to test the performance of the method in random noise attenuation and signal restoration.

Theory

Spatial projection-based complex empirical mode decomposition

EMD is widely used in time–frequency analysis. EMD stabilizes a nonstationary signal by decomposing it into IMFs. The stationary IMFs satisfy two conditions (Huang et al., 1998): 1) the number of extremes and zero crossings in the dataset must be either equal or differ by one at most, and 2) the mean value of the envelope defined by the local maxima and the local minima is zero at all points. Each IMF has a relatively local constant frequency. Most seismic signals are nonlinear and nonstationary, and the aim of applying EMD is to decompose the nonstationary signals into stationary components of different frequency ranges.

Traditional EMD cannot deal with complex signals directly; thus, it divides a complex signal into real and imaginary parts and decomposes them independently. This decomposition not only destroys the unity of the complex signals but also leads to inconsistent decomposition numbers.

In this paper, the CEMD algorithm based on spatial projection (Rilling et al., 2007) is used to directly decompose complex signals. This method considers a complex signal as fast oscillations superimposed by slower oscillations. Projection vectors are obtained by projecting the complex signal on different directions. The slow oscillations can be extracted by using the mean of the envelope of the extremes of all projection vectors, and then the fast oscillation can be obtained by subtracting the slow oscillations from the original signal. This method achieves the direct decomposition of a complex signal and avoids the inconsistency between real and imaginary decomposition. Moreover, the resultant CIMFs can reflect the different oscillations embedded in the original complex signal. Figure 1 shows the CEMD, and the detailed steps of the algorithm are the following (Rilling et al., 2007).

1) Project the complex signal $x(t)$ on a given direction $\varphi_k (1 \le k \le N)$ to obtain the projection vector

$$p_{\phi_k}\left(t\right) = \mathrm{Re}(e^{-i\phi_k} x(t)), \tag{1}$$

where i denotes the imaginary unit and N denotes the number of projection directions.

2) Extract the values and locations of maxima of $p_{\varphi_k}(t)$ in the specific direction φ_k and then interpolate them to obtain the envelope $e_{\varphi_k}(t)$.

3) Repeat steps 1 to 2 for all projection directions and calculate the mean value $m(t)$ of all envelopes by equation (2)

$$m(t) = \frac{1}{N}\sum_k e_{\phi_k}\left(t\right). \tag{2}$$

4) Subtract the mean value $m(t)$ from the original signal $x(t)$ and determine if the residual satisfies the aforementioned two conditions of IMF. If it does, the residual can be treated as an IMF. If not, the residual will be treated as the original signal, and steps 1 to 3 should

be repeated until the two conditions are satisfied. At this point, the first CIMF is obtained.

5) Subtract the first CIMF from the original signal $x(t)$ and treat the residual as a new signal. Repeat the decomposition process until it becomes either a monotonic function or a constant. Finally, a series of CIMFs will be obtained.

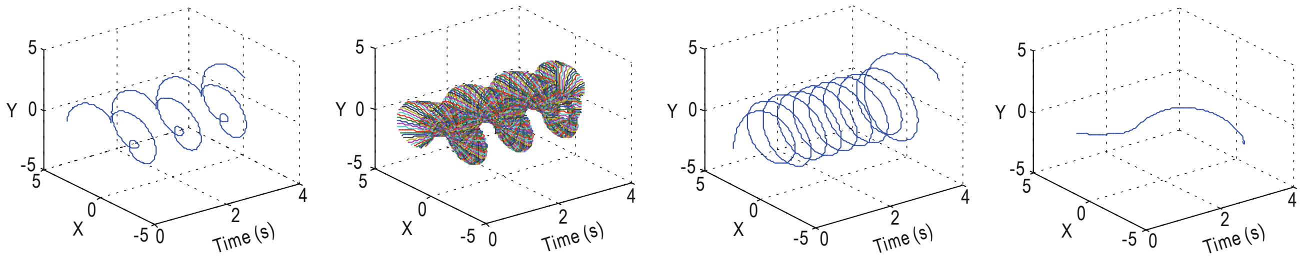

(a) The original complex-valued signal

(b) Envelopes of the projection vectors at different directions

(c) Fast oscillation

(d) Residual slow oscillation

Fig.1 Demonstration of CEMD on a synthetic signal.

F–x spatial projection-based complex empirical mode decomposition predictive filtering

The FXEMD denoising method, proposed by Bekara and van der Baan (2009), has many successful applications; however, simply subtracting the first IMF will result in signal damage and limited denoising ability because signals coexist with random noise in all IMFs. In addition, decomposing the real and imaginary parts may lead to inconsistent decomposition numbers of real and imaginary parts, which consequently makes the reconstitution of complex signals more difficult.

To solve these problems, a novel random noise attenuation method named FXCEMDdecon is proposed. First, the nonstationary seismic data are decomposed into stationary CIMFs by using the spatial projection-based CEMD algorithm, and then, random noise attenuation on all CIMFs is carried out by using the FXdecon method. The process comprises the following steps.

1) Assume that the 2D seismic data in the frequency–space (f–x) domain can be expressed as $\hat{s}(f,x)$.

2) Decompose a given frequency slice $\hat{s}(f_u,x)$ along the spatial direction by using the spatial projection-based CEMD algorithm to obtain the CIMFs $\hat{m}_{cimfs}(f_u,x)$, which satisfy the two conditions mentioned above.

3) Derive the prediction operator a_l with the following equation

$$\hat{m}_{cimfs}(f_u,n)=\sum_{l=1}^{p}a_l*\hat{m}_{cimfs}(f_u,n-l), \tag{3}$$

where n denotes the number of seismic traces and p denotes the prediction step. The filtered frequency slice $\hat{\hat{s}}(f_u,x)$ can be obtained by stacking all the filtered CIMFs.

4) Repeat steps 2 and 3 for all frequency slices to obtain the filtered data $\hat{\hat{s}}(f,x)$.

5) Transform the filtered data $\hat{\hat{s}}(f,x)$ to the t–x domain to obtain the final denoising results.

Synthetic examples

Figure 2 shows a synthetic complex signal consisting of three frequency components. The blue solid curve corresponds to the real part and the red dashed curve to the imaginary part. The synthetic signal is decomposed by using the conventional EMD and spatial projection-based CEMD method, and the results are shown in Figure 3 using the same symbols. Figures 3a–3b show the three CIMFs and Figure 3d shows the residuals using the conventional EMD method. Figures 3e–3g show the three CIMFs and Figure 3h shows the residuals using the CEMD method. The three CIMFs obtained with the conventional EMD method significantly deviate from the three frequency components of the original signal. Especially, for the imaginary part, it only appears in the first CIMF but disappears in the second and third CIMF. The inconsistency between the real and imaginary IMF numbers may potentially damage the unity of complex signals in noise attenuation using the EMD method. In contrast to the conventional EMD method, the three CIMFs obtained by using the spatial projection-based CEMD method are consistent with the three frequency components of the original signal in magnitude and frequency.

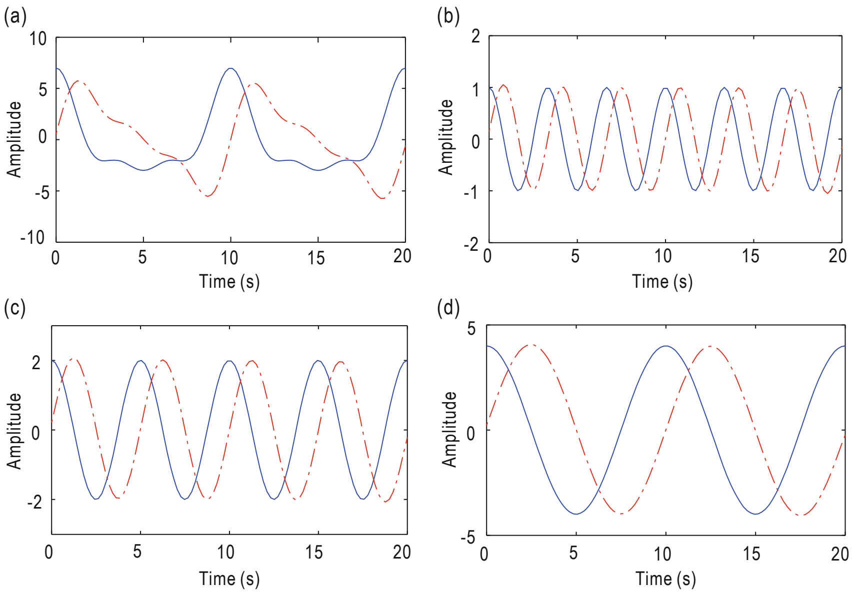

Fig.2 Synthetic complex signal (a) and its three frequency components (b)–(d). Solid curve denotes the real part and the dotted curve denotes the imaginary part.

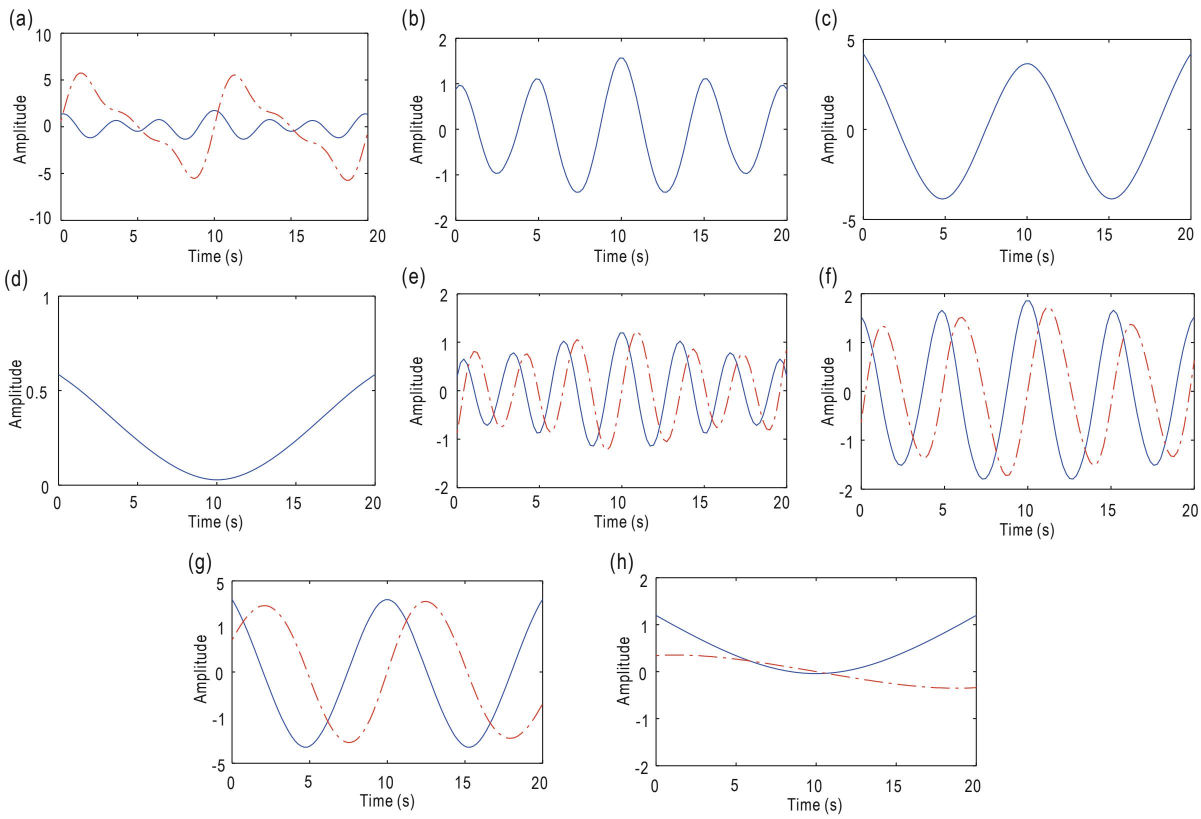

Fig.3 EMD on the synthetic signal: (a)–(c) CIMFs and (d) residual using the conventional EMD decomposition method; and (e)–(g) CIMFs and (h) residual using the spatial projection-based decomposition method.

Next, synthetic seismic data are used to test the algorithm. The noise-free synthetic data are shown in Figure 4a, whereas Figure 4b shows the 25% noise-added section. The synthetic data contain 20 traces and the offset is from 0 m to 100 m with a 5 m interval. The total time record of the trace is 1 s and the time interval is 4 ms. To test the signal preservation ability of the algorithm, two types of events are used, including a horizontal event with maximum amplitude of one and two conflicted events with maximum amplitude of two, which correspond to a weak and complex signal. Then, the FXCEMDdecon, FXEMD, and FXdecon methods are used to remove the noise, and the results are shown in Figures 5, 6, and 7, respectively. For convenience, we also calculate the frequency–wavenumber (F–K) spectra of the noise attenuation results for FXCEMDdecon, FXEMD, and FXdecon, which are shown in Figures 8c–8e, respectively. From Figure 5 and the F–K spectrum (Figure 8c), we can see that the proposed FXCEMDdecon method has good denoising performance. The majority of the reflection and weak signals are preserved in the denoising section, whereas little of the effective signal remains on the removed noise profile. From Figure 7, we can see that the FXdecon poorly preserves the weak signal because the horizontal reflection disappears in the denoising section (Figure 7a). This phenomenon is also seen in the F–K spectrum (Figure 8e). Although the noise attenuation results obtained with FXEMD are better than the results with FXdecon, residual signals of conflicting events remain on the noise section (Figure 6b). In addition, by comparing the F–K spectra in Figures 8a and 8d, we see that the effective signals become weak for wavenumbers between −0.05 and 0.05. When the wavenumbers are larger than 0.05 and smaller than −0.05, the energy of the effective signals almost disappears. This implies that the FXEMD method is equivalent to a binary filter in the wavenumber domain, and it destroys the dip event if the process window is not appropriately selected. This issue will be discussed later. In real seismic data processing,

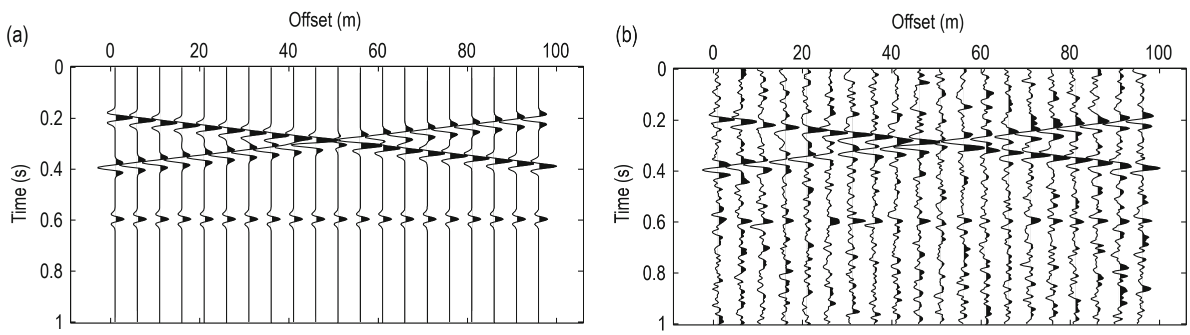

Fig.4 Synthetic data: (a) noise-free synthetic data and (b) data with 25% Gaussian noise added.

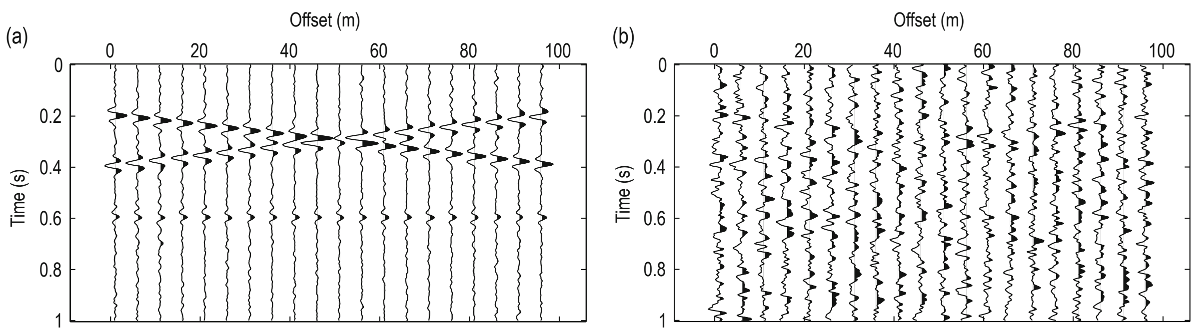

Fig.5 Noise attenuation using the FXCEMDdecon method (a) and the removed noise section (b).

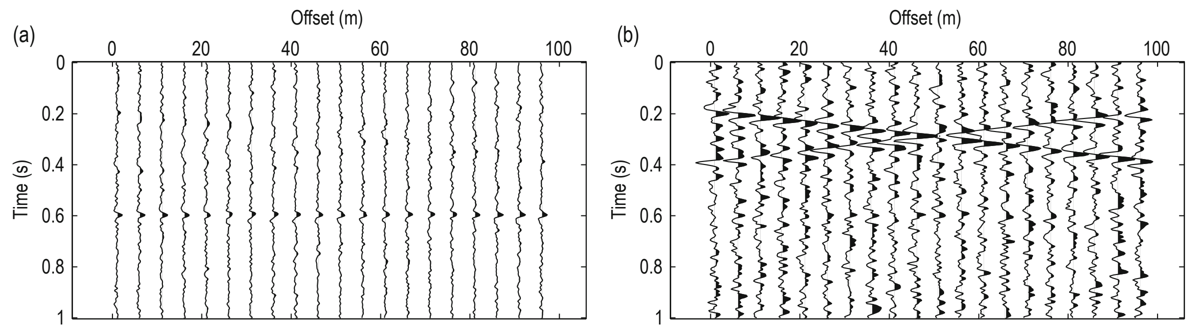

Fig.6 Noise attenuation using the FXEMD method (a) and the removed noise section (b).

random noise attenuation is mainly used to embellish poststack data. Serious damage to weak reflections and minor fault reflections will result in misinterpretations. Hence, all results confirm that the proposed scheme offers the best noise attenuation performance.

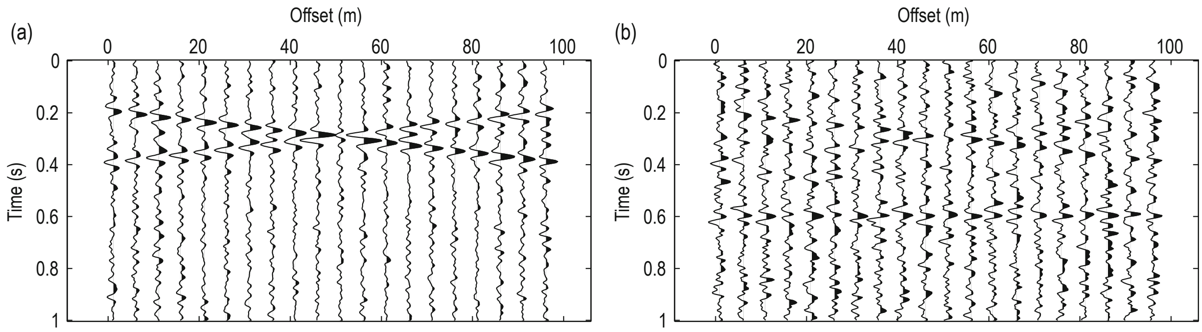

Fig.7 Noise attenuation using the FXdecon method (a) and the removed noise section (b).

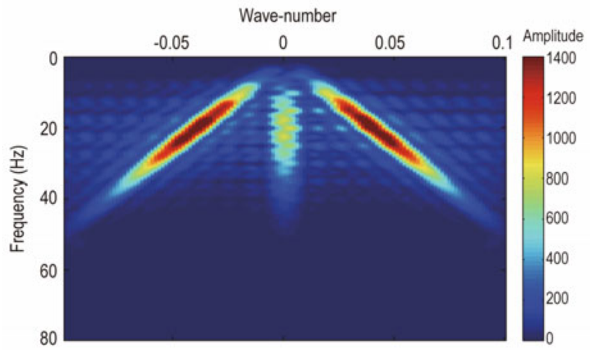

(a) Noise-free synthetic data

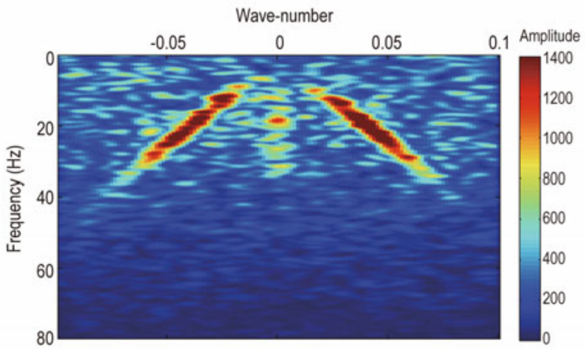

(b) Noisy synthetic data

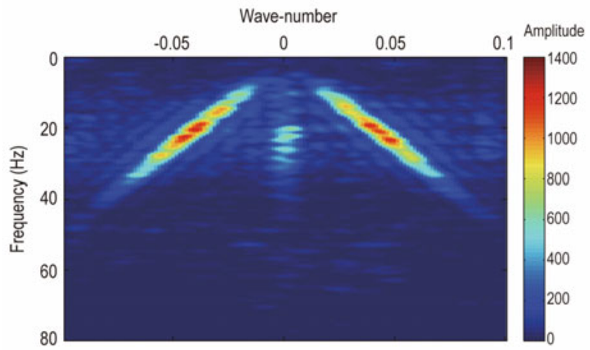

(c) denoising results with the FXCEMDdecon method

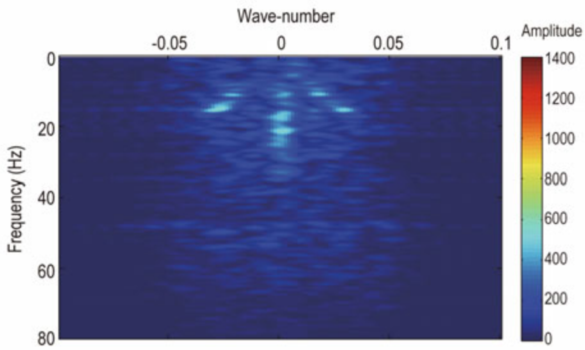

(d) denoising results with the FXEMD method

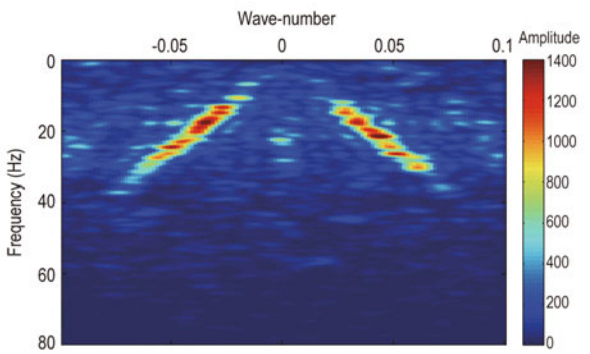

(e) denoising results with the FXdecon method

Fig.8 Comparison of F–K spectra.

Next, the superiority of the FXCEMDdecon method is examined. From the spectrum of IMFs for white Gaussian noise in Figure 9, we can see that the frequency range of IMFs decreases by half, which suggests that EMD is equivalent to a binary filter, and this feature does not change as the data length changes (Rilling et al., 2007). Therefore, when the FXEMD approach is used, subtracting the first IMF will only lead to an effective signal between lower wavenumber ranges. When the signals of the most conflicting events are outside the half-range of the original wavenumbers, the effective signals are destroyed. Therefore, FXEMD is not appropriate to process seismic data when steep events exist. A feasible solution is to select and process a small lateral time window.

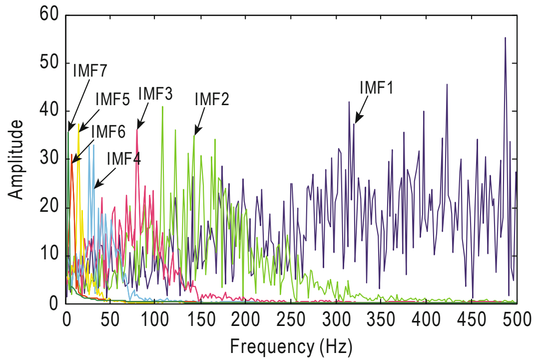

Fig.9 Spectra of IMFs for white Gaussian noise.

The FXdecon method is essentially a dip filter in the *f*–*x* domain (Gulunay, 1986). It is based on the assumption that seismic events have the same slope. When different slope events appear in the seismic section, signals with strong energy significantly contribute to the filter operator, whereas signals with weak energy (particularly with energy close to noise) contribute little. Thus, the calculated filter operator will attenuate the weak signals as noise, resulting in signal energy loss.

The FXCEMDdecon method offers two advantages. First, CEMD makes seismic data more suitable for FXdecon. Second, considered as an oscillation with specific frequency, each CIMF has a relatively single slope. When the FXdecon is used in CIMFs, different slope events can be filtered, and the errors owing to mixtures of dipping events are avoided. Therefore, the proposed FXCEMDdecon method has the best signal preservation performance.

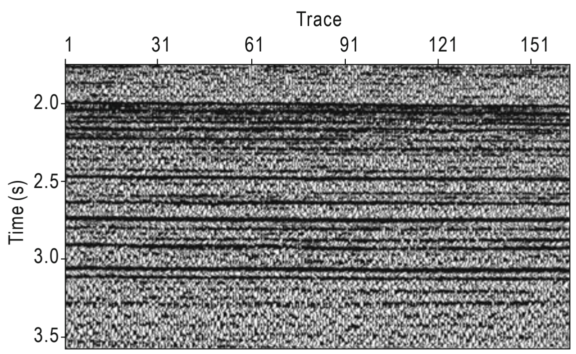

Fig.10 Original seismic profile from western China.

Field data example

The proposed method is applied to field seismic data of carbonate reservoirs in western China. Random noise is common in seismic profiles and overlaps with the effective signals in the frequency range. The SNR of the seismic data is small largely because of the noise. The random noise attenuation directly affects the final processing results.

To demonstrate the denoising effect, we choose a seismic profile with low SNR. As shown in Figure 10, seismic events have poor continuity, and the signals are weak. Figures 11a, 11b, and 11c show the noise attenuation profiles of the FXCEMDdecon, FXEMD, and FXdecon methods. We can see that FXCEMDdecon method offers the best noise attenuation and signal preservation. In particular, for the weak event around 2.2 s and 2.6 s as well as the discontinuous events below the strong event around 2.7 s (marked by the ellipses), the FXCEMDdecon method preserves the weak reflections and enhances the continuity of events. Though the FXEMD method uses the EMD algorithm to decompose nonstationary seismic data into stationary IMFs, simply subtracting the first CIMF will result in signal loss and will prevent the random noise attenuation in the other IMFs. The FXdecon method directly processes nonstationary seismic data and hardly achieves ideal amplitude-preserving denoising. Clearly, the FXCEMDecon method has two advantages over the FXEMD and FXdecon methods.

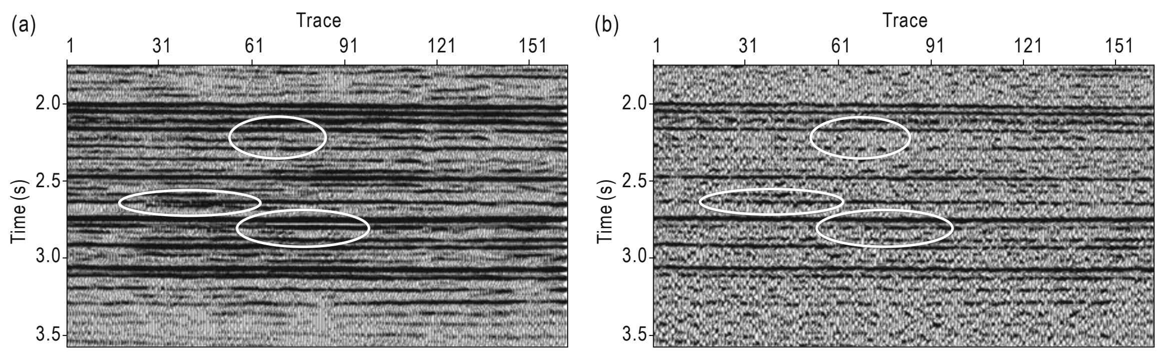

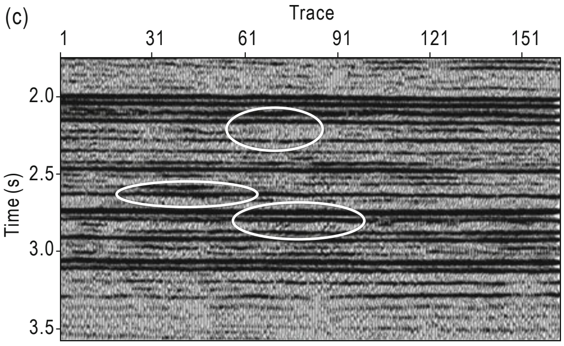

Fig.11 Noise attenuation with the FXCEMDdecon (a), FXEMD (b), and FXdecon (c).

Conclusions

Seismic data become complex when transferred to the frequency domain from the time domain. The unity of complex signals may be damaged when noise detection and attenuation is independently applied to the real and imaginary parts of a complex signal. We improve the conventional EMD-based noise attenuation method by directly using CEMD and applying FXdecon to all CIMFs. The method can be treated as an extension of conventional EMD in combination with the FXdecon method. Synthetic and real seismic data were used to verify the performance of the method in random noise attenuation and seismic signal restoration.

References

Abma, R., and Claerbout, J., 1995, Lateral prediction for noise attenuation by *t*−*x* and *f*−*x* techniques: Geophysics, **60**(6), 1887–1896.

Battista, B. M., Knapp, C., McGee, T., and Goebel, V., 2007, Application of the empirical mode decomposition and Hilbert-Huang transform to seismic reflection data: Geophysics, **72**(2), 29–37.

Bekara, M., and van der Baan, M., 2009, Random and coherent noise attenuation by empirical mode decomposition: Geophysics, **74**(5), 89–98.

Canales, L. L., 1984, Random noise reduction: 54th Annual International Meeting, SEG, Expanded Abstracts, 525–527.

Gulunay, N., 1986, FXDECON and complex Wiener prediction filter: 56th Annual International Meeting, SEG, Expanded Abstracts, 279–281.

Huang, N. E., Shen, Z., Long, S. R., Wu, M. C., Shih, H. H., Zheng, Q., Yen, N. C., Tung, C. C., and Liu, H. H., 1998, The empirical mode decomposition and the Hilbert spectrum for nonlinear and non-stationary time series analysis: Proceedings of the Royal Society of London. Series A: Mathematical, Physical and Engineering Sciences, **454**(1971), 903–995.

Ioup, J. W., and Ioup, G. E., 1998, Noise removal and compression using a wavelet transform: 68th Annual International Meeting, SEG, Expanded Abstracts, 1076–1079.

Rilling, G., Flandrin, P., Goncalves, P., and Lilly, J. M., 2007, Bivariate Empirical Mode Decomposition: IEEE Signal Processing Letters, **14**(12), 936–939.

Sacchi, M. D., and Kuehl, H., 2001, ARMA formulation of FX prediction error filters and projection filters: Journal of Seismic Exploration, **9**(3), 185–197.

Soubaras, R., 1994, Signal-preserving random noise attenuation by the *f*–*x* projection: 64th Annual International Meeting, SEG, Expanded Abstracts, 1576–1579.

Trickett, S. R., 2003, F-xy eigenimage noise suppression: Geophysics, **68**(2), 751–759.

Wang, D. L., Tong, Z. F., Tang, C., and Zhu, H., 2010, An iterative curvelet thresholding algorithm for seismic random noise attenuation: Applied Geophysics, **7**(4), 315–324.

Yuan, S. Y., and Wang, S. X., 2011, A local *f*–*x* Cadzow method for noise reduction of seismic data obtained in complex formations: Petroleum Science, **8**(3), 269–277.

Ma Yan-Yan received a BS (2007) in Information and Computing Science and a MS (2011) in Earth Exploration and Information Technology from China University of Petroleum (Beijing). She is presently a Ph.D. candidate in China University of Petroleum (Beijing), majoring in Geological Resources and Geological Engineering. Her research interests are seismic data processing and reservoir prediction.